Critical behavior and magnetocaloric effect in Mn_{3}Si_{2}Te_{6}

Yu Liu (□□) and C. Petrovic

Phys. Rev. B **98**, 064423 — Published 27 August 2018

DOI: 10.1103/PhysRevB.98.064423

Critical behavior and magnetocaloric effect in $Mn_3Si_2Te_6$

Yu Liu (刘育) and C. Petrovic
Condensed Matter Physics and Materials Science Department, Brookhaven National Laboratory, Upton, New York 11973, USA
(Dated: August 13, 2018)

The critical properties and magnetocaloric effect of semiconducting ferrimagnet $Mn_3Si_2Te_6$ single crystals have been investigated by bulk magnetization and heat capacity around T_c. Critical exponents $\beta = 0.41 \pm 0.01$ with a critical temperature $T_c = 74.18 \pm 0.08$ K and $\gamma = 1.21 \pm 0.02$ with $T_c = 74.35 \pm 0.05$ K are deduced by the Kouvel-Fisher plot, whereas $\delta = 4.29 \pm 0.05 (3.40 \pm 0.02)$ is obtained by a critical isotherm analysis at $T = 74(75)$ K. The magnetic exchange distance is found to decay as $J(r) \approx r^{-4.79}$, which lies between the mean-field and 3D Heisenberg models. Moreover, the magnetic entropy change $-\Delta S_M$ features a maximum at T_c, i.e., $-\Delta S_M^{max} \sim 2.53(1.67)$ J kg^{-1} K^{-1} with in-plane(out-of-plane) field change of 5 T, confirming large magnetic anisotropy. The heat capacity measurement further gives $-\Delta S_M^{max} \sim 2.94$ J kg^{-1} K^{-1} and the corresponding adiabatic temperature change $\Delta T_{ad} \sim 1.14$ K with out-of-plane field change of 9 T.

I. INTRODUCTION

Layered intrinsically ferromagnetic (FM) semiconductors hold great promise for both fundamental physics and applications in spintronic devices.[?] [?] [?] [?] [?] CrI_3 has recently attracted much attention since the long-range magnetism persists in monolayer with T_c of 45 K.[?] Intriguingly, the magnetism in CrI_3 is layer-dependent, from FM in monolayer, to antiferromagnetic (AFM) in bilayer, and back to FM in trilayer.[?] It can further be controlled by electrostatic doping, providing great opportunities for designing magneto-optoelectronic devices.[?] [?]

Ternary $Cr_2X_2Te_6$ (X = Si, Ge) exhibit FM order below T_c of 32 K for $Cr_2Si_2Te_6$ and 61 K for $Cr_2Ge_2Te_6$, respectively,[?] [?] [?] [?] [?] and also promising candidates for long-range magnetism in nanosheets.[?] [?] [?] Many efforts have been devoted to shed light on the nature of FM in this system.[?] [?] [?] [?] [?] [?] [?] Multiple domain structure types, self-fitting disks and fine ladder structure within the Y-connected walls, were observed by magnetic force microscopy,[?] confirming two-dimensional (2D) long-range magnetism with non-negligible interlayer coupling.[?] $Mn_3Si_2Te_6$ is a little-studied three-dimensional (3D) analog of $Cr_2Si_2Te_6$.[?] [?] [?] The $Mn_2Si_2Te_6$ layer is composed of $MnTe_6$ octahedra that are edge sharing within the *ab* plane (Mn1 site) and along with Si-Si dimers [Fig. 1(a)], similar to $Cr_2Si_2Te_6$. However, the layers are connected by filling one-third of Mn atoms at the Mn2 site within interlayer, yielding a composition of $Mn_3Si_2Te_6$.[?] Recent neutron diffraction experiment gives that $Mn_3Si_2Te_6$ is a ferrimagnet below $T_c \approx 78$ K and the moments lie within the *ab* plane.[?]

In the present work we investigated the critical behavior of $Mn_3Si_2Te_6$ single crystal by using modified Arrott plot, Kouvel-Fisher plot and critical isotherm analysis, as well as its magnetocaloric effect. Critical exponents $\beta = 0.41(1)$ with $T_c = 74.18(8)$ K, $\gamma = 1.21(2)$ with $T_c = 74.35(5)$ K, and $\delta = 4.29(5)$ at $T = 74$ K. The magnetic exchange distance is found to decay as $J(r) \approx r^{-4.79}$, which lies between mean-field and 3D Heisenberg models. The rescaled $-\Delta S_M(T, H)$ curves can well collapse onto a universal curve, confirming its nature of second-order.

II. METHODS

A. Experimental details

Single crystals of $Mn_3Si_2Te_6$ were fabricated by melting stoichiometric mixture of Mn (3N, Alfa Aesar) chip, Si (5N, Alfa Aesar) lump and Te (5N, Alfa Aesar) shot. Starting materials were vacuum-sealed in a quartz tube, heated to 1100 °C over 20 h and then cooled to 850 °C at a rate of 1 °C/h. X-ray diffraction (XRD) data were taken with Cu K_α ($\lambda = 0.15418$ nm) radiation of a Rigaku Miniflex powder diffractometer. The magnetization and heat capacity were collected in Quantum Design MPMS-XL5 and PPMS-9 systems. The magnetic entropy change $-\Delta S_M$ from the magnetization data was estimated using a Maxwell relation.

B. Scaling analysis

According to the scaling hypothesis, the second-order phase transition around the Curie point T_c is characterized by a set of interrelated critical exponents α, β, γ, δ, η, ν and a magnetic equation of state.[?] The exponent α can be obtained from specific heat and β and γ from spontaneous magnetization M_s and inverse initial susceptibility χ_0^{-1}, below and above T_c, respectively, while δ is the critical isotherm exponent. The mathematical definitions of the exponents from magnetization measurement are given below:

$$M_s(T) = M_0(-\varepsilon)^\beta, \varepsilon < 0, T < T_c, \quad (1)$$

$$\chi_0^{-1}(T) = (h_0/m_0)\varepsilon^\gamma, \varepsilon > 0, T > T_c, \quad (2)$$

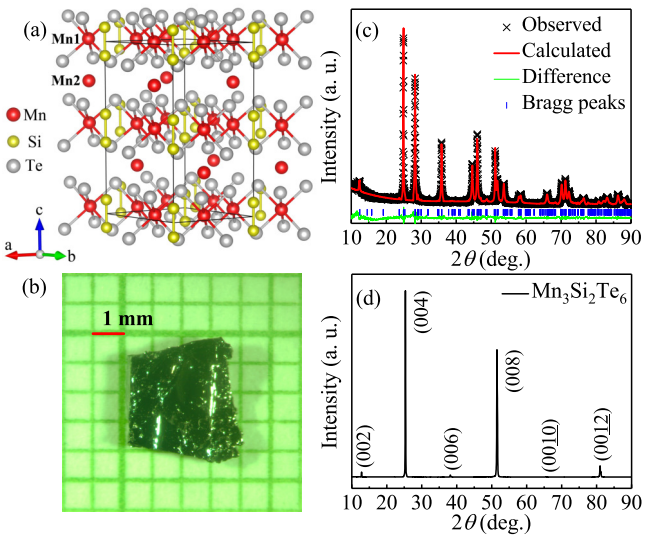

FIG. 1. (Color online) (a) Crystal structure and (b) representative single crystal of $Mn_3Si_2Te_6$. (c) Powder x-ray diffraction (XRD) and (d) single-crystal XRD patterns of $Mn_3Si_2Te_6$ at room temperature. The vertical tick marks represent Bragg reflections of the $P\bar{3}1c$ space group.

$$M = DH^{1/\delta}, T = T_c, \tag{3}$$

where $\varepsilon = (T - T_c)/T_c$ is the reduced temperature, and M_0, h_0/m_0 and D are the critical amplitudes.[?]

The magnetic equation of state in the critical region is expressed as

$$M(H, \varepsilon) = \varepsilon^{\beta} f_{\pm}(H/\varepsilon^{\beta+\gamma}), \tag{4}$$

where f_+ for $T > T_c$ and f_- for $T < T_c$, respectively, are the regular functions. Eq.(4) can be further written in terms of scaled magnetization $m \equiv \varepsilon^{-\beta} M(H, \varepsilon)$ and scaled field $h \equiv \varepsilon^{-(\beta+\gamma)} H$ as

$$m = f_{\pm}(h). \tag{5}$$

This suggests that for true scaling relations and the right choice of β, γ, and δ values, scaled m and h will fall on universal curves above T_c and below T_c, respectively.

III. RESULTS AND DISCUSSIONS

The powder XRD pattern of $Mn_3Si_2Te_6$ confirms high purity of the single crystals, in which the observed peaks can be well fitted with the $P\bar{3}1c$ space group [Fig. 1(c)]. The determined lattice parameters $a = 7.046(2)$ Å and $c = 14.278(2)$ Å are very close to the reported values.[? ?] In the single-crystal XRD [Fig. 1(d)], only $(00l)$ peaks are detected, indicating that the crystal surface is parallel to the ab plane and perpendicular to the c axis.

Figure 2 presents the temperature dependence of magnetization measured in $H = 1$ and 50 kOe applied in the ab plane and parallel to the c axis, respectively. The

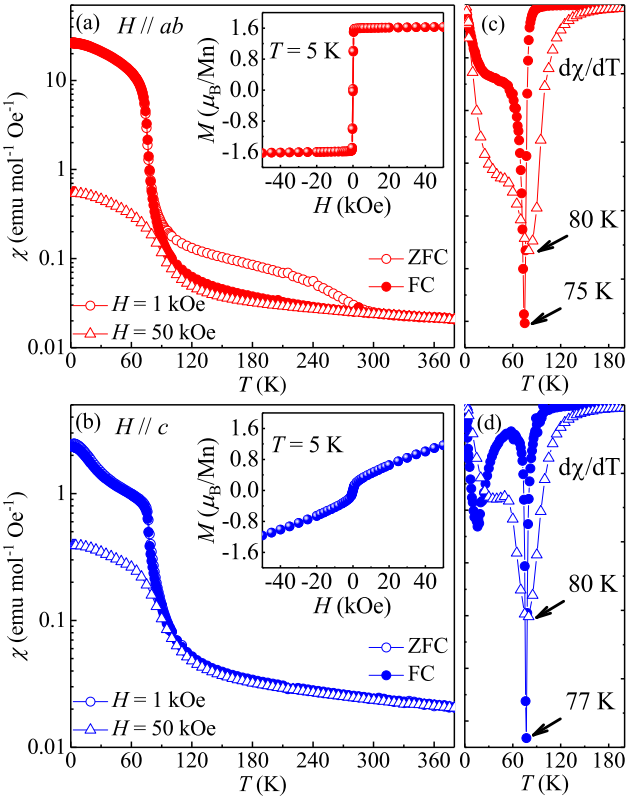

FIG. 2. (Color online) Temperature dependence of dc magnetic susceptibility χ and corresponding $d\chi/dT$ for $Mn_3Si_2Te_6$ measured in the magnetic field $H = 1$ and 50 kOe applied (a,c) in the ab plane and (b,d) along the c axis, respectively. Insets: field dependence of magnetization measured at $T = 5$ K.

magnetization is nearly isotropic in 50 kOe, however, significant magnetic anisotropy is observed in 1 kOe at low temperatures. The ordered moments lie primarily within the ab plane. An additional upturn well above T_c till to 300 K is clearly seen in zero-field-cooling (ZFC) curve for **H//ab**, which may be associated with short-range order or the presence of correlated excitations in the paramagnetic region.[?] Isothermal magnetization at $T = 5$ K [insets in Fig. 2] shows saturation moment of $M_s \approx 1.6$ μ_B/Mn for **H//ab** and a small FM component for **H//c**. No remanent moment for either orientation confirms the crystal of high quality. The T_c can be roughly determined by the minimum of $d\chi/dT$ [Figs. 2(c,d)], i.e., $T_c = 75$ K for in-plane field and $T_c = 77$ K for out-of-plane field of 1 kOe, which shifts to $T_c = 80$ K in an increase field of 50 kOe.[?]

From the Landau theory of phase transition, the Gibbs free energy G for FM-paramagnetic(PM) transition can be expressed as

$$G(T, M) = G_0 + aM^2 + bM^4 - MH, \tag{6}$$

where the equilibrium magnetization M is the order parameter, and the coefficients a and b are the temperature-dependent parameters. At equilibrium $\partial G/\partial M = 0$ (i.e.,

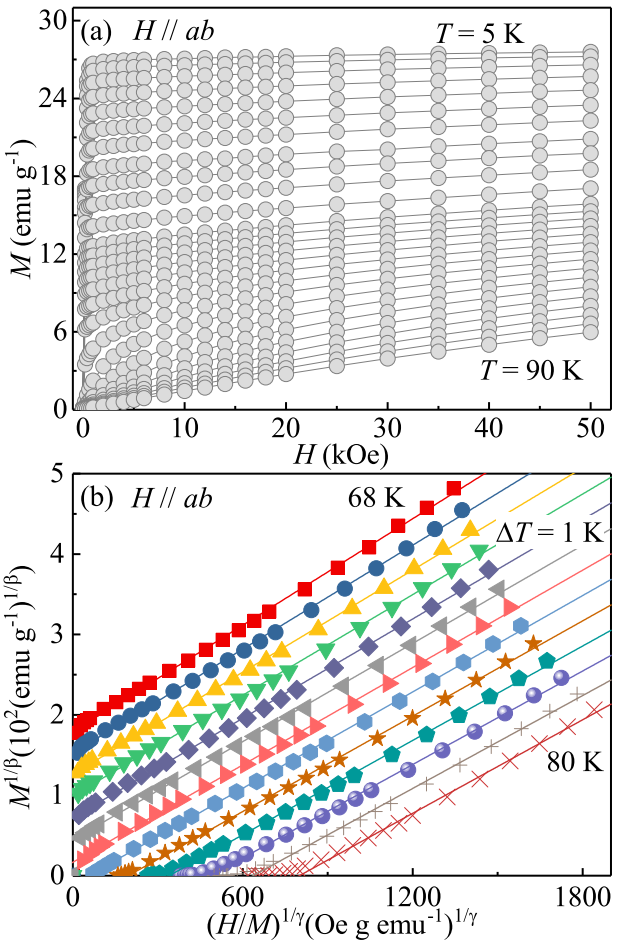

FIG. 3. (Color online) (a) Typical initial isothermal magnetization curves measured in **H**//**ab** from 5 to 90 K for $Mn_3Si_2Te_6$. (b) the modified Arrott Plot around T_c for the optimum fitting with $\beta = 0.41$ and $\gamma = 1.21$.

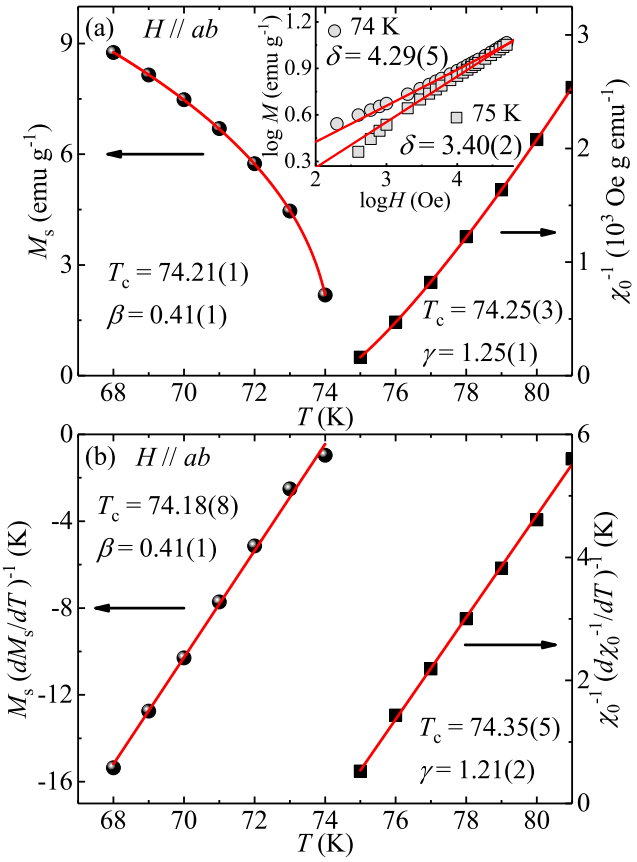

FIG. 4. (Color online) (a) Temperature dependence of the spontaneous magnetization M_s (left) and the inverse initial susceptibility χ_0^{-1} (right) with solid fitting curves. Inset shows log$M$ vs log$H$ collected at 74 and 75 K with linear fitting curves. (b) Kouvel-Fisher plots of $M_s(dM_s/dT)^{-1}$ (left) and $\chi_0^{-1}(d\chi_0^{-1}/dT)^{-1}$ (right) with solid fitting curves.

energy minimization) and the magnetic equation of state can be expressed as

$$H/M = 2a + 4bM^2. \quad (7)$$

Thus, the Arrott plot of M^2 vs H/M should appear as parallel straight lines for different temperatures above and below T_c in the high field region.[?] The intercepts of M^2 on the H/M axis is negative or positive depending on phenomena below or above T_c and the line at T_c passes through the origin. In order to properly determine the T_c as well as the critical exponents β, γ, and δ, the modified Arrott plot with a self-consistent method was used.[? ?] Figure 3 presents the initial isotherms ranging from 5 to 90 K and the modified Arrott plot of $M^{1/\beta}$ vs $(H/M)^{1/\gamma}$ around T_c for $Mn_3Si_2Te_6$. This gives $\chi_0^{-1}(T)$ and $M_s(T)$ as the intercepts on the H/M axis and positive M^2 axis, respectively.

Figure 4(a) exhibits the final $M_s(T)$ and $\chi_0^{-1}(T)$ as a function of temperature. According to Eqs. (1) and (2), the critical exponents $\beta = 0.41(1)$ with $T_c = 74.21(1)$ K, and $\gamma = 1.25(1)$ with $T_c = 74.25(3)$ K, are obtained. In addition, there is also the Kouvel-Fisher (KF) relation,[?]

$$M_s(T)[dM_s(T)/dT]^{-1} = (T - T_c)/\beta, \quad (8)$$

$$\chi_0^{-1}(T)[d\chi_0^{-1}(T)/dT]^{-1} = (T - T_c)/\gamma. \quad (9)$$

Linear fittings to the plots of $M_s(T)[dM_s(T)/dT]^{-1}$ and $\chi_0^{-1}(T)[d\chi_0^{-1}(T)/dT]^{-1}$ vs T in Fig. 4(b) yield $\beta = 0.41(1)$ with $T_c = 74.18(8)$ K, and $\gamma = 1.21(2)$ with $T_c = 74.35(5)$ K. The third exponent δ can be calculated from the Widom scaling relation $\delta = 1 + \gamma/\beta$. From β and γ obtained with the modified Arrott plot and the Kouvel-Fisher plot, $\delta = 4.05(5)$ and 3.95(2) are obtained, respectively, which are close to the direct fits of δ taking into account that $M = DH^{1/\delta}$ near T_c [$\delta = 4.29(5)$ at 74 K and 3.40(2) at 75 K, inset in Fig. 4(a)].

Scaling analysis can be used to estimate the reliability of the obtained critical exponents and T_c. From Eq. (5), scaled m vs scaled h, all the data collapse on two separate branches below and above T_c, as depicted in Fig. 5. The

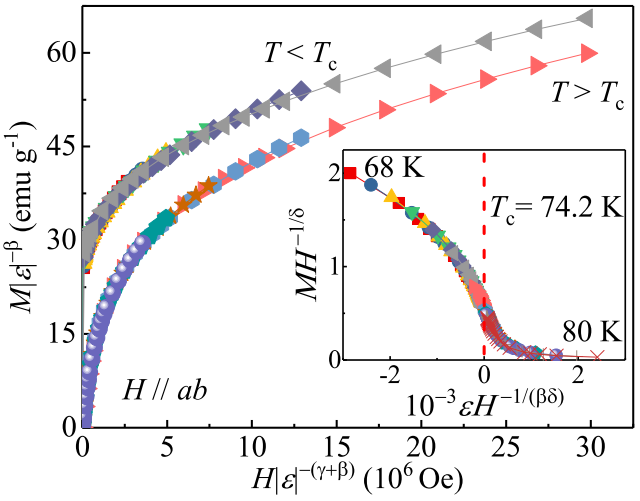

FIG. 5. (Color online) Scaled magnetization m vs scaled field h below and above T_c for $Mn_3Si_2Te_6$. Inset: the rescaling of the $M(H)$ curves by $MH^{-1/\delta}$ vs $\varepsilon H^{-1/(\beta\delta)}$.

scaling equation of state takes another form,

$$\frac{H}{M^{\delta}} = k\left(\frac{\varepsilon}{H^{1/\beta}}\right), \tag{10}$$

where $k(x)$ is the scaling function. From Eq. (10), all the data should also fall into a single curve. This is indeed seen [inset in Fig. 5]; the $MH^{-1/\delta}$ vs $\varepsilon H^{-1/(\beta\delta)}$ experimental data for $Mn_3Si_2Te_6$ collapse into a single curve and the T_c locates at the zero point of the horizontal axis. The well-rescaled curves further confirm the reliability of the obtained critical exponents.

Next, it is important to understand the nature as well as the range of interaction in this material. In a homogeneous magnet the universality class of the magnetic phase transition depends on the exchange distance $J(r)$. In renormalization group theory analysis the interaction decays with distance r as

$$J(r) \approx r^{-(3+\sigma)}, \tag{11}$$

where σ is a positive constant.[?] Moreover, the susceptibility exponent γ is predicted as

$$\gamma = 1 + \frac{4}{d}\left(\frac{n+2}{n+8}\right)\Delta\sigma + \frac{8(n+2)(n-4)}{d^2(n+8)^2} \times \left[1 + \frac{2G(\frac{d}{2})(7n+20)}{(n-4)(n+8)}\right]\Delta\sigma^2, \tag{12}$$

where $\Delta\sigma = (\sigma - \frac{d}{2})$ and $G(\frac{d}{2}) = 3 - \frac{1}{4}(\frac{d}{2})^2$, n is the spin dimensionality.[?] When $\sigma > 2$, the Heisenberg model is valid for 3D isotropic magnet, where $J(r)$ decreases faster than r^{-5}. When $\sigma \leq 3/2$, the mean-field model is satisfied, expecting that $J(r)$ decreases slower than $r^{-4.5}$. In the present case, $\sigma = 1.79$, then the correlation length critical exponent $\nu = 0.676$ ($\nu = \gamma/\sigma$), and α = -0.028

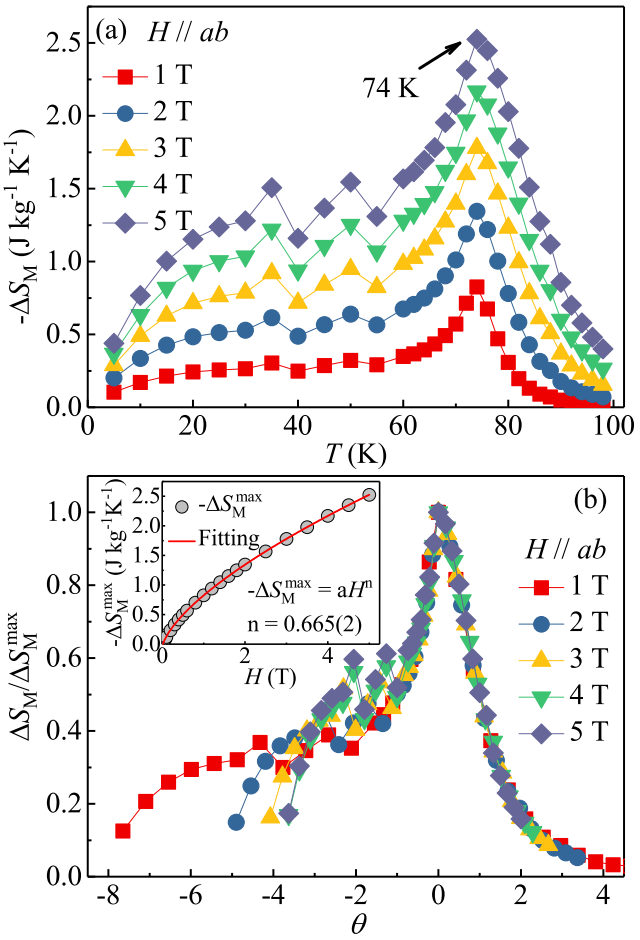

FIG. 6. (Color online) (a) The magnetic entropy change $-\Delta S_M$ obtained from magnetization at various magnetic fields change in the ab plane. (b) Normalized ΔS_M as a function of the rescaled temperature θ. Inset: magnetic field dependence of the maximum magnetic entropy change $-\Delta S_M^{max}$ with power law fitting in red solid line.

($\alpha = 2 - \nu d$). It is found that the magnetic exchange distance decays as $J(r) \approx r^{-4.79}$, which lies between that of 3D Heisenberg model and mean-field model.

Then we estimate its magnetic entropy change

$$\Delta S_M(T,H) = \int_0^H \left[\frac{\partial S(T,H)}{\partial H}\right]_T dH. \tag{13}$$

With the Maxwell's relation $\left[\frac{\partial S(T,H)}{\partial H}\right]_T = \left[\frac{\partial M(T,H)}{\partial T}\right]_H$, it can be further written as:[?]

$$\Delta S_M(T,H) = \int_0^H \left[\frac{\partial M(T,H)}{\partial T}\right]_H dH. \tag{14}$$

In the case of magnetization measured at small discrete magnetic field and temperature intervals [Fig. 3(a)],

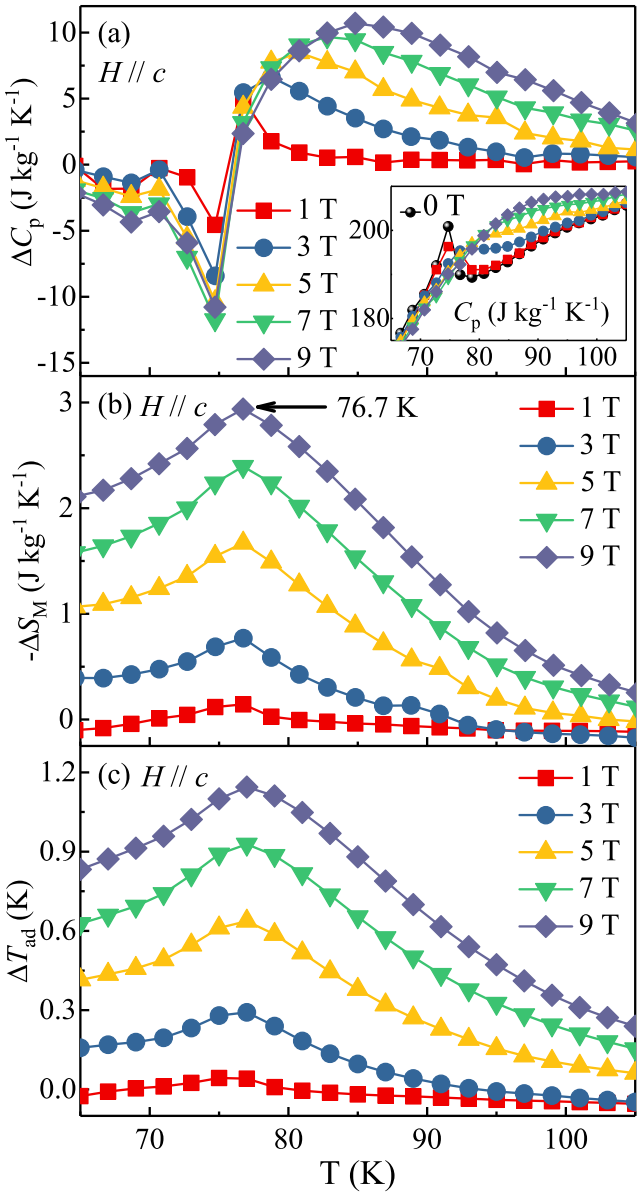

FIG. 7. (Color online) Temperature dependences of (a) the specific heat change ΔC_p, (b) the magnetic entropy change $-\Delta S_M$ and (c) the adiabatic temperature change ΔT_{ad} for $Mn_3Si_2Te_6$ at the indicated fields. Inset shows the temperature dependence of specific heat C_p.

$\Delta S_M(T,H)$ could be practically approximated as,

$$\Delta S_M(T_i,H) = \frac{\int_0^H M(T_i,H)dH - \int_0^H M(T_{i+1},H)dH}{T_i - T_{i+1}}. \quad (15)$$

Figure 6(a) gives the calculated $-\Delta S_M$ as a function of temperature. All the $-\Delta S_M(T,H)$ curves present a pronounced peak at T_c, and the peak broads asymmetrically on both sides with increasing field. The maximum value of $-\Delta S_M$ reaches 2.53 J kg^{-1} K^{-1} with in-plane field change of 5 T. This is comparable to $Mn_{2-x}Cr_xSb$ but smaller than in $MnFeP_{0.45}As_{0.55}$ or $Gd_5Ge_2Si_2$ magnetic refrigerant materials.[? ?]

Scaling analysis of $-\Delta S_M$ can be built by normalizing all the $-\Delta S_M$ curves against the respective maximum $-\Delta S_M^{max}$, namely, $\Delta S_M/\Delta S_M^{max}$ by rescaling the temperature θ as defined in the following equations,[?]

$$\theta_- = (T_{peak} - T)/(T_{r1} - T_{peak}), T < T_{peak}, \quad (16)$$

$$\theta_+ = (T - T_{peak})/(T_{r2} - T_{peak}), T > T_{peak}, \quad (17)$$

where T_{r1} and T_{r2} are the temperatures of the two reference points that have been selected as those corresponding to $\Delta S_M(T_{r1},T_{r2}) = \frac{1}{2}\Delta S_M^{max}$. Following this method, all the $-\Delta S_M(T,H)$ curves in various fields collapse into a single curve in the vicinity of T_c [Fig. 6(b)]. In the framework of the mean-field theory, $-\Delta S_M^{max} = -1.07qR(g\mu_B JH/k_BT_c)^{2/3} \propto H^{2/3}$, where q is the number of magnetic ions, R is the gas constant, and g is the Lande factor.[?] In fact, more universally, it should follow a power law relation, $-\Delta S_M^{max} = aH^n$, where n depends on the magnetic state of the sample. Fitting of the field dependence of $-\Delta S_M^{max}$ with $\mathbf{H//ab}$ gives $n = 0.665(2)$ [inset in Fig. 6(b)], close to the typical value of 2/3 within mean-field model.

Finally, we also estimate the $-\Delta S_M$ from heat capacity measurement with out-of-plane fields up to 9 T. The λ peak observed at $T_c = 74.7$ K in zero field [inset in Fig. 7(a)], corresponding well to the PM-FM transition, is gradually suppressed in fields. Figure 7(a) shows the calculated heat capacity change $\Delta C_p = C_p(T,H) - C_p(T,0)$ as a function of temperature in various fields. Obviously, $\Delta C_p < 0$ for $T < T_c$ and $\Delta C_p > 0$ for $T > T_c$, whilst, it changes sharply from negative to positive at T_c, corresponding to the change from FM to PM. The entropy $S(T,H)$ can be deduced by

$$S(T,H) = \int_0^T \frac{C_p(T,H)}{T} dT. \quad (18)$$

Assuming the electronic and lattice contributions are not field dependent and in an adiabatic process of changing the field, the magnetic entropy change $-\Delta S_M$ can be straightly obtained $-\Delta S_M(T,H) = S_M(T,H) - S_M(T,0)$. The adiabatic temperature change ΔT_{ad} caused by the field change can be obtained by $\Delta T_{ad}(T,H) = T(S,H) - T(S,0)$, where $T(S,H)$ and $T(S,0)$ are the temperatures in the field $H \neq 0$ and $H = 0$, respectively, at constant total entropy $S(T,H)$. Figures 7(b) and 7(c) exhibit the temperature dependence of $-\Delta S_M$ and ΔT_{ad} estimated from heat capacity with out-of-plane field. The maxima of $-\Delta S_M$ and ΔT_{ad} increase with increase field and reach the values of 2.94 J kg^{-1} K^{-1} and 1.14 K, respectively, with the field change of 9 T.

IV. CONCLUSIONS

In summary, we have studied the critical behavior and magnetocaloric effect around the FM-PM transition in

$Mn_3Si_2Te_6$ single crystal. The ferrimagnetic transition in $Mn_3Si_2Te_6$ is identified to be second order in nature. The critical exponents β, γ, and δ estimated from various techniques match reasonably well and follow the scaling equation, suggesting a long-range magnetic interaction with the exchange distance decaying as $J(r) \approx r^{-4.79}$. Magnetocaloric effect is about one order of magnitude smaller when compared to other magnetorefrigerant candidate materials.

ACKNOWLEDGEMENTS

This work was supported by the US DOE-BES, Division of Materials Science and Engineering, under Contract No. DE-SC0012704 (BNL).

[1] M. A. McGuire, G. Clark, S. KC, W. M. Chance, G. E. Jellison, Jr., V. R. Cooper, X. D. Xu, and B. C. Sales, Phys. Rev. M **1** 014001 (2017).

[2] M. A. McGuire, H. Dixit, V. R. Cooper, and B. C. Sales, Chem. Mater. **27**, 612 (2015).

[3] B. Huang, G. Clark, E. Navarro-Moratalla, D. R. Klein, R. Cheng, K. L. Seyler, D. Zhong, E. Schmidgall, M. A. McGuire, D. H. Cobden, W. Yao, D. Xiao, P. Jarillo-Herrero, and X. D. Xu, Nature **546**, 270 (2017).

[4] C. Gong, L. Li, Z. L. Li, H. W. Ji, A. Stern, Y. Xia, T. Cao, W. Bao, C. Z. Wang, Y. Wang, Z. Q. Qiu, R. J. Cava, S. G. Louie, J. Xia, and X. Zhang, Nature **546**, 265 (2017).

[5] K. L. Seyler, D. Zhong, D. R. Klein, S. Guo, X. Zhang, B. Huang, E. Navarro-Moratalla, L. Yang, D. H. Cobden, M. A. McGuire, W. Yao, D. Xiao, P. Jarillo-Herrero, and X. D. Xu, Nature Physics **14**, 277 (2018).

[6] S. Jiang, L. Li, Z. Wang, K. F. Mak, and J. Shan, arXiv:1802.07355.

[7] B. Huang, G. Clark, D. R. Klein, D. MacNeill, E. Navarro-Moratalla, K. L. Seyler, N. Wilson, M. A. McGuire, D. H. Cobden, D. Xiao, W. Yao, P. Jarillo-Herrero, and X. D. Xu, arXiv:1802.06979.

[8] G. Ouvrard, E. Sandre, and R. Brec, J. Solid State Chem. **73**, 27 (1988).

[9] V. Carteaux, G. Ouvrard, J. C. Grenier, and Y. Laligant, J. Magn. Magn. Mater. **94**, 127 (1991).

[10] V. Carteaux, D. Brunet, G. Ouvrard, and G. André, J. Phys.: Condens. Matter **7**, 69 (1995).

[11] L. D. Casto, A. J. Clune, M. O. Yokosuk, J. L. Musfeldt, T. J. Williams, H. L. Zhuang, M. W. Lin, K. Xiao, R. G. Hennig, B. C. Sales, J. Q. Yan, and D. Mandrus, APL Mater. **3**, 041515 (2015).

[12] X. Zhang, Y. L. Zhao, Q. Song, S. Jia, J. Shi, and W. Han, Jpn. J. Appl. Phys. **55**, 033001 (2016).

[13] H. L. Zhuang, Y. Xie, P. R. C. Kent, and P. Ganesh, Phys. Rev. B **92**, 035407 (2015).

[14] M. W. Lin, H. L. Zhuang, J. Q. Yan, T. Z. Ward, A. A. Puretzky, C. M. Rouleau, Z. Gai, L. B. Liang, V. Meunier, B. G. Sumpter, P. Ganesh, P. R. C. Kent, D. B. Geohegan, D. G. Mandrus, and K. Xiao, J. Mater. Chem. C, **4**, 315 (2016).

[15] X. X. Li, and J. L. Yang, J. Mater. Chem. C, **2**, 7071 (2014).

[16] X. F. Chen, J. S. Qi, and D. N. Shi, Phys. Lett. A, **379**, 60 (2015).

[17] N. Sivadas, M. W. Daniels, R. H. Swendsen, S. Okamoto, and D. Xiao, Phys. Rev. B, **91**, 235425 (2015).

[18] J. P. Liu, S. Y. Park, K. F. Garrity, and D. Vanderbilt, Phys. Rev. Lett., **117**, 257201 (2016).

[19] B. J. Liu, Y. M. Zou, L. Zhang, S. M. Zhou, Z. Wang, W. K. Wang, Z. Qu, and Y. H. Zhang, Sci. Rep. **6**, 33873 (2016).

[20] G. T. Lin, H. L. Zhuang, X. Luo, B. J. Liu, F. C. Chen, J. Yan, Y. Sun, J. Zhou, W. J. Lu, P. Tong, Z. G. Sheng, Z. Qu, W. H. Song, X. B. Zhu, and Y. P. Sun, Phys. Rev. B **95**, 245212 (2017).

[21] Y. Liu and C. Petrovic, Phys. Rev. B **96**, 054406 (2017).

[22] T. F. Guo, Z. W. Ma, G. T. Lin, X. Luo, Y. B. Hou, Y. P. Sun, Z. G. Sheng, and Q. Y. Lu, arXiv:1803.06113.

[23] R. Rimet, C. Schlenker, and H. Vincent, J. Magn. Magn. Mater. **25**, 7 (1981).

[24] H. Vincent, D. Leroux, D. Bijaoui, R. Rimet, and C. Schlenker, J. Solid State Chem. **63**, 349 (1986).

[25] A. F. May, Y. Liu, S. Calder, D. S. Parker, T. Pandey, E. Cakmak, H. Cao, J. Yan, and M. A. McGuire, Phys. Rev. B **95**, 174440 (2017).

[26] H. E. Stanley, *Introduction to Phase Transitions and Critical Phenomena* (Oxford U. P., London and New York, 1971).

[27] M. E. Fisher, Rep. Prog. Phys. **30**, 615 (1967).

[28] A. Arrott, Phys. Rev. B **108**, 1394 (1957).

[29] W. Kellner, M. Fähnle, H. Kronmüller, and S. N. Kaul, Phys. Status Solidi B **144**, 387 (1987).

[30] A. K. Pramanik, and A. Banerjee, Phys. Rev. B **79**, 214426 (2009).

[31] J. S. Kouvel, and M. E. Fisher, Phys. Rev. **136**, A1626 (1964).

[32] M. E. Fisher, S. K. Ma, and B. G. Nickel, Phys. Rev. Lett. **29** 917 (1972).

[33] S. F. Fischer, S. N. Kaul, and H. Kronmuller, Phys. Rev. B **65**, 064443 (2002).

[34] J. Amaral, M. Reis, V. Amaral, T. Mendonc, J. Araujo, M. Sa, P. Tavares, J. Vieira, J. Magn. Magn. Mater. **290**, 686 (2005).

[35] L. Caron, F. Miao, J. C. P. Klaasse, S. Gama and E. Brück, Appl. Phys. Lett. **103**, 112404 (2013).

[36] O. Tegus, E. Brück, K. H. J. Buschow and F. R. de Boer, Nature **415**, 150 (2002).

[37] V. Franco and A. Conde, Int. J. Refrig. **33**, 465 (2010).

[38] H. Oesterreicher and F. T. Parker, J. Appl. Phys. **55**, 4334 (1984).